PREPRINT

Early-life stress alters chromatin modifications in VTA to prime stress sensitivity

Luke T. Geiger[1,6,‡], Julie-Anne Balouek[1,‡], Lorna A. Farrelly[2], Andy S. Chen[1], Megan Tang[1], Shannon N. Bennett[1], Eric J. Nestler[2], Benjamin A. Garcia[3], Ian Maze[2,4,5], Catherine Jensen Peña[1*]

ABSTRACT:

Early-life stress increases sensitivity to subsequent stress, which has been observed among humans, other animals, at the level of cellular activity, and at the level of gene expression. However, the molecular mechanisms underlying such long-lasting sensitivity are poorly understood. We tested the hypothesis that persistent changes in transcription and transcriptional potential were maintained at the level of the epigenome, through changes in chromatin. We used a combination of bottom-up mass spectrometry, viral-mediated epigenome-editing, behavioral quantification, and RNA-sequencing in a mouse model of early-life stress, focusing on the ventral tegmental area (VTA), a brain region critically implicated in motivation, reward learning, stress response, and mood and drug disorders. We find that early-life stress in mice alters histone dynamics in VTA and that a majority of these modifications are associated with an open chromatin state that would predict active, primed, or poised gene expression, including enriched histone-3 lysine-4 methylation and the H3K4 monomethylase *Setd7*. Mimicking ELS through over-expression of *Setd7* and enrichment of H3K4me1 in VTA recapitulates ELS-induced behavioral and transcriptional hypersensitivity to future stress. These findings enrich our understanding of the epigenetic mechanisms linking early-life environmental experiences to long-term alterations in stress reactivity within the brain's reward circuitry, with implications for understanding and potentially treating mood and anxiety disorders in humans.

INTRODUCTION

Early-life stress (ELS) increases lifetime risk for anxiety, depression, and substance use disorders (Green et al., 2010; Kendler et al., 2011; Scott et al., 2012). The brain's reward circuitry functions at the intersection of both negative and positive valence domains and is extensively implicated in the pathophysiology of mood and anxiety disorders (Russo and Nestler, 2013; Hanson et al., 2021) and is therefore an ideal target for better understanding the functional consequences of ELS within the brain. Indeed, ELS exerts prominent and long-lasting effects within brain reward regions in clinical and preclinical studies (Cabib et al., 1993; Brake et al., 2004; Hanson et al., 2015, 2016; Marusak et al., 2017; Shepard and Nugent, 2020; Spyrka et al., 2020; Park et al., 2021) including long-lasting alterations in transcription and epigenetic programming (Authement et al., 2015; Lepack et al., 2016; Peña et al., 2017, 2019b; Marrocco et al., 2019; Shepard et al., 2020; Kronman et al., 2021). Using RNA-sequencing, we and other previously examined changes in transcription resulting from ELS, adult stress, or a combination of the two across ventral tegmental area (VTA), nucleus accumbens (NAc), prefrontal cortex, and hippocampus in male and female mice and found both long-lasting changes in transcription following ELS and gene expression changes that were primed by ELS and revealed by a second hit of adult stress (Peña et al., 2017, 2019b; Kos et al., 2023). We hypothesize that these persistent changes in transcription and transcriptional potential in VTA are maintained at the level of the epigenome through changes in chromatin.

Chromatin dynamically responds to developmental and environmental cues, acts as a substrate of molecular memory in cells, and facilitates adaptive gene expression responses

[1] Princeton Neuroscience Institute, Princeton University, Princeton, NJ
[2] Nash Family Department of Neuroscience, Friedman Brain Institute, Icahn School of Medicine at Mount Sinai, New York, NY
[3] Department of Biochemistry and Molecular Biophysics, Washington University School of Medicine, St. Louis, MO
[4] Department of Pharmacological Sciences, Icahn School of Medicine at Mount Sinai, New York, NY
[5] Howard Hughes Medical Institute, Icahn School of Medicine at Mount Sinai, New York, NY
[6] Present address: Department of Biological Sciences, Columbia University, New York, NY

‡ These authors contributed equally to this work
* Correspondance to: Catherine J. Peña (cpena@princeton.edu)

to recurring stimuli, a phenomenon known as epigenetic priming (Calo and Wysocka, 2013; D'Urso and Brickner, 2017; Lämke and Bäurle, 2017). Post-translational histone modifications (PTHMs), including methylation, acetylation, OGlyc-NAc, serotonylation, and dopaminylation have been implicated in a wide variety of psychiatric diseases and are altered in response to acute and chronic stress across the lifespan (Covington et al., 2011; Levine et al., 2012; Howerton et al., 2013; Heller et al., 2014; Pusalkar et al., 2015; Sun et al., 2015; Lepack et al., 2016, 2020; Bastle and Maze, 2019; Farrelly et al., 2019; Morrison et al., 2020; Kronman et al., 2021; Torres-Berrío et al., 2023). However, the complexity of the histone code is enormous (Jenuwein and Allis, 2001) and work to-date on ELS-induced histone modifications in VTA has been limited to profiling of only a few PTHMs of interest (Shepard et al., 2018).

Our recent work in NAc supports a hypothesized role for chromatin in mediating the impact of ELS: we identified dynamic changes in dozens of chromatin modifications across the lifespan in NAc of male and female mice and causally related key changes to adult stress sensitivity (Lepack et al., 2016; Kronman et al., 2021). Here, we extend these chromatin findings to the VTA, the dopaminergic hub of the brain's reward circuitry. We used bottom-up mass spectrometry to characterize approximately 200 individual and combinatorial PTHMs in adult VTA following ELS. We then determined whether changes in PTHMs could be driven by changes in corresponding histone-modifying enzymes, and homed in on the histone-3 lysine-4 monomethyltransferase *Setd7*. Finally, we tested the hypothesis that elevated levels of H3K4me1 during development are sufficient to prime sensitivity to future stress at both behavioral and gene expression levels, thereby mimicking ELS.

METHODS

Mice

C57BL/6J mice were maintained on a 12 h light/dark cycle (lights on at 4 am) with *ad libitum* access to food and water. All experiments were conducted in accordance with the guidelines of the Institutional Animal Care and Use Committee at Mount Sinai (histone modification study) and Princeton University (qPCR and *Setd7* studies). Virgin males and females were obtained (Jackson) and bred in-house in trios, males removed after 3-5 days, and females separated to individual cages 20 days after breeding.

Early life stress (ELS)

Litters were randomly assigned at birth to standard-facility rearing (Std) or early life stress (ELS) conditions. ELS was performed from postnatal day P10-17 as previously described (Peña et al., 2017, 2019b, 2019a). Briefly, ELS consisted of 3-4 hours of maternal separation at random times during the light cycle wherein all pups from a litter were removed to a clean holding cage and in addition, EnviroDri nesting material in the home cage was reduced to approximately ½ of standard-reared cages during the days of separations and then restored. Pups were weaned at P21 into cages by litter and sex and left undisturbed except for regular cage changes and checks. Adult male mice were used for the histone profiling experiment. Both males and females were included in *Setd7* experiments. Retired Swiss-Webster male breeder mice (Taconic) were housed individually and used as aggressor mice in chronic non-discriminatory social defeat stress.

Transgene expression in juvenile mice

Standard-reared male and female pups were randomly assigned to either experimental *Setd7*-over-expression group or a control GFP group. At P14 (behavior) or P28 (protein validation), C57BL6/J mice were anesthetized with isoflurane (2-3% induction; 1-3% maintenance) for surgeries and fitted into dual-arm stereotax. P14 pups were installed with the nose fitted in the nose cone above the bite bar, and the head stabilized using blunt ends of ear bars between the ear and jaw. To bilaterally target the VTA, two Hamilton syringes were angled inward 7˚, the Bregma-Lambda distance was measured, the Lambda was taken as the starting point. The following coordinates were used: ML: ± 0.7 mm, AP: +0.86 mm from Lambda, DV: -4.2 mm (P14), or ML: ± 1 mm, AP: +0.91 mm from Lambda, DV: -4.6 mm (P28). 300 nL of AAV (1.9 x 1013) were injected on each side for P14 and 500 nL for P28. Both VetBond glue and two sterile sutures were used to ensure complete healing of incisions. Mice were given a perioperative topical dose of bupivacaine (0.25%, 2 mg/kg) and an additional dose 24h following surgery. Mice recovered in a partially-warmed cage before being returned to their home cage. To prevent cannibalization of P14 pups by dams following surgery, dams were habituated with a piece of paper towel with sterile eye lubricant (Puralube Vet Ointment Sterile Ocular Lubricant, Dechra) and liquid tissue adhesive (VetBond, 3M); pups were only returned to the home cage with the dam once completely ambulatory. No qualitative differences in coat quality, grooming, gross locomotor behavior, or water drinking were detectable during testing following surgery. Mice were then aged to adulthood (P60-70) in standard housing conditions.

Adult stress: chronic non-discriminatory social defeat stress

In order to test whether epigenetic priming by SETD7-driven H3K4me1 enrichment enhances stress sensitivity, male and female mice were exposed to either control conditions or mild "non-discriminatory" social defeat stress ("defeat") during the light phase (Yohn et al., 2019), as previously described (Balouek et al., 2023). Briefly, male

and female mice experienced daily social defeat by a Swiss Webster retired breeder ("aggressor;" Taconic) together for 5 days. Female mice were then tested for behavior while male mice experienced 5 more days of social defeat, without a female present, based on previous work documenting that as few as 4 days of adult stress in females is sufficient to induce similar behavioral changes as chronic stress in males (Hodes et al., 2015; Muir et al., 2020). On each day of social defeat, an experimental male mouse was introduced to an aggressor's cage (standard rat cage filled with corncob bedding) first for ~3 minutes, then an experimental female mouse was added into the cage for an additional 5 minutes. Males were then moved across a perforated plexiglass barrier within the aggressor cage, while females were single-housed in a separate rat cage, with a handful of soiled aggressor bedding. Experimental mice were introduced to a new aggressor each day, and males and females rotated in different directions so that trios were unique each day. However, aggressor mice in these experiments were observed to attack less overall on days when females were present, and thus the adult stressor was considered mild for these experiments compared to the standard ten days of male-only social defeat stress. Control mice were housed in a standard mouse cage in pairs of the same sex, separated by a perforated plexiglass barrier.

Behavioral testing

Social avoidance: One day after the last day of social defeat stress, mice were assessed for social avoidance in a social interaction test as previously described (Peña et al., 2017). Social avoidance has been associated with other depression-like behaviors and is responsive to antidepressant treatment (Berton et al., 2006; Krishnan et al., 2007). The test was performed in two stages: during the first 2.5 min, each experimental mouse freely explored an arena (44 x 44 x 20 cm) containing an enclosure centered against one wall of the arena made of plexiglass and wire mesh (10 x 6 cm). The experimental mouse was then returned to its homecage while a novel Swiss-Webster mouse (aggressive retired male breeder) was placed into the enclosure. The experimental mouse was then immediately returned to the arena and allowed to explore the arena freely for 2.5 min. Time spent in the 'interaction zone' (14×26 cm) surrounding the enclosure, 'corner zones' (10×10 cm), and 'distance traveled' within the arena was measured by video tracking software (Ethovision, Noldus). A social interaction ratio (SI Ratio) was calculated as time spent exploring the novel mouse over time exploring the novel enclosure object. Mice were considered "susceptible" to social defeat if SI Ratio <0.8, "resilient" if SI Ratio >1.2, and "indifferent" for interaction scores in between.

Open-field test: Exploratory and anxiety-like behavior was measured by open field exploration one day after social interaction testing. For 10 minutes, mice were allowed to freely explore an empty arena (44 x 44 x 20 cm). Total distance traveled, velocity and time spent in the center (20 x 20 cm) were recorded and measured by video tracking software (Ethovision, Noldus), as previously described (Peña et al., 2017).

Novelty-suppressed feeding: One day following open-field testing, female mice were tested for anxiety- and depression-like behavior in the novelty-suppressed feeding test. Novelty suppressed feeding testing was adapted from previous work (Bodnoff et al., 1989; Samuels and Hen, 2011). Eighteen hours prior to testing, mice were moved to a clean homecage without food; water was provided *ad libitum*. Testing happened in the dark phase of the circadian cycle. Mice were placed in a corner of a novel, brightly-lit (200 lux) arena (44 x 44 x 20 cm). The floor was covered with a novel bedding (corncob) and a single food pellet was placed onto a white circular platform (10 cm diameter) in the center of the arena. The test was stopped as soon as mice took their first bite (sitting on their haunches and using their forepaws to hold and bite the pellet), or after a maximum of 10 minutes. Mice that timed out were assigned a latency of 600 seconds. Immediately after taking their first bite, mice were transferred to their home cages and given access to their usual amount of food. The time to eat in the homecage was also recorded and a ratio of time to first bite in the arena over time to first bite in the homecage was calculated to measure anxiety-like behavior.

Histological and Molecular Methods

Tissue collection for histone modification profiling and RNA extraction

Brains were harvested from adult mice by cervical dislocation and rapid removal into ice-cold PBS. Using an ice-cold slice matrix, bilateral 1 mm-thick 16 gauge punches of VTA were taken fresh and flash-frozen in tubes on dry ice. For mass spectrometry, bilateral VTA tissue punches from three male mice were pooled into a single tube for each sample for processing. Pups from the same litter were combined whenever possible, and pups from different litters of the same condition (Std vs ELS) were pooled otherwise. For RNA extraction (qPCR or sequencing), each sample consisted of tissue from a single male or female mouse.

Histone purification and bottom-up mass spectrometry

Three pooled samples were used from each condition (n=3 each for Std and ELS, no adult stress). Extraction of histones and preparation of MS-ready samples were performed as described (Bhanu et al., 2020). Briefly, histones were extracted in acid from isolated chromatin and purified by TCA precipitation and acetone wash. The purified histones were estimated using Bradford assay and approximately 10-20ug was used to derivatize unmodified lysines, in a mixture of propionic anhydride and acetonitrile (1:3 ratio v/v) for 20 minutes at room temperature. This was

followed by digestion with 1μg trypsin/20 ug of histones, 6 hours to overnight at room temperature. Subsequently, derivatization was repeated to propionylate all free N-termini of the peptides. These samples were desalted prior to LC-MS analysis using C18 Stage-tips. Peptide concentration was measured using BCA assay to inject same amount of sample peptides. Quantification of histone peptides were performed in nanoLC coupled online to an LTQ-Orbitrap Elite mass spectrometer (Thermo Scientific). About 1-5 μg of desalted samples were then separated using a 75 μm ID x 17 cm Reprosil-Pur C18-AQ (3 μm; Dr. Maisch GmbH, Germany) nano-column mounted on an EASY-nLC nanoHPLC (Thermo Scientific, San Jose, Ca, USA) in a gradient of 2% to 28% solvent B (A = 0.1% formic acid; B = 95% MeCN, 0.1% formic acid) over 45 minutes, from 28% to 80% solvent B in 5 minutes, 80% B for 10 minutes at a flow-rate of 300 nL/min. and data were acquired using data-independent acquisition (DIA). Briefly, full scan MS (m/z 300–1100) was acquired in the Orbitrap with a resolution of 120,000 (at 200 m/z) and an AGC target of 5x10e5. MS/MS was performed in the ion trap with sequential isolation windows of 50 m/z with an AGC target of 3x10e4, a CID collision energy of 35 and a maximum injection time of 50 msec. MS/MS data were collected in centroid mode.

Statistical analysis for mass-spec

For quantification, total area under the extracted ion chromatograms (AUC) were considered for each PTM-bearing peptide and its unmodified form. This was expressed as relative ratio (AUC of any form of the peptide to sum of AUCs of all forms of the peptides with the same amino acid sequence, both modified and unmodified). For isobaric peptides, the relative ratio of two isobaric forms was estimated by averaging the ratio for each fragment ion with different mass between the two species. Within each sample and for each peptide fragment, the proportion of unmodified or modified peptide was calculated by summing mass-spec areas of all modified peptides in that fragment and calculating simple ratios from the total.

Alterations in histone PTHM proportions at each peptide residue were visualized as parts of a whole given their proportional dependency. Because proportions of modifications at each histone fragment are not independent, we performed repeated measures ANOVA to assess interactions between rearing condition and proportion of modifications. Post-hoc two-tailed Student's t-tests were used to assess differences in fold-change at each histone modification between Std and ELS groups, as previously described (Lepack et al., 2016). All significance thresholds were set at $p<0.05$; $p<0.1$ was considered trend-level.

RNA extraction

On the day following behavioral testing, mice were sacrificed by rapid cervical dislocation. Brains were rapidly removed, and bilateral 1 mm-thick 16 gauge punches of VTA were taken fresh, flash-frozen on dry ice, and stored at -80C until processing. RNA was extracted from tissue samples with Trizol (Invitrogen) and chloroform (Sigma) and purified with RNeasy Micro Kits (Qiagen). Separate cohorts of mice were used for qPCR and sequencing experiments. For qPCR experiments, tissue and cDNA was used from a previous study (Bennett et al., 2024).

qPCR

For relative quantification of histone methyltransferases in VTA after ELS, cDNA was created with a reverse-transcription kit (HighCapRT, Applied Biosystems). Primers for real-time semi-quantitative PCR (qPCR) were validated for efficiency and specificity. The following primer pairs were used: *Setd7* (Forward: GCAGGGCCAGGGCGTTTACA; Reverse: GGCCGGTCCATTCAGCTCTCC); *Kmt2a* (also known as MLL1; Forward: TGCTAAAGGGAACTTCTGCCC; Reverse: TCTCATCTTCTGTACCTGAGAGACT); *Hprt* (as housekeeping gene; Forward: GCAGTACAGCCCCAAAATGG; Reverse: GGTCCTTTTCACCAGCAAGCT). All qPCR reactions were run in triplicate and used SYBR-green on a QuantStudio 7 (ThermoFisher). The 2^(-ΔΔCt) method was used to calculate RNA expression analysis compared to the standard-reared group (including both males and females) with *Hprt* as a control reference gene (Livak and Schmittgen, 2001). In addition, we similarly calculated relative expression changes from normalized reads of published RNA-seq data from male VTA [Gene Expression Omnibus (GEO) accession GSE89692; (Peña et al., 2017)] for histone-modifying genes of interest.

RNA-sequencing

We analyzed changes in gene expression across the transcriptome by RNA-sequencing following viral-mediated *Setd7* or *Gfp* expression, social defeat, and behavioral testing. RNA was converted into libraries for RNA-sequencing using an Illumina TruSeq RiboZero kit. Samples each reflect one individual mouse, except for one sample in which two female *Setd7*-CNSDS mice were combined due to insufficient RNA concentration. After confirming the quality of the cDNA library, it was sequenced for paired-end reads to a read depth of over 15 million (15M) reads per sample at the Lewis-Sigler Institute for Integrative Genomics (Princeton University).

RNA-seq data analysis

Reads from the Illumina TruSeq RNA library were analyzed using the Galaxy Genomics platform. Quality checks were performed using FastQC. Reads were then mapped to a reference mouse genome (GRCm39) using Bowtie2. Using the FeatureCounts tool, the mapped reads were counted across mouse genes and assessed for gene body coverage to check for potential bias in the quantity or quality

of reads along the genome. Principal component analysis by DESeq2 identified one male *Setd7*-CNSDS mouse sample as an outlier, and the sample was removed from further analysis. Thus, for our final DEG analysis, we used 7 male samples (2 *Gfp*-Ctrl, 2 *Setd7*-Ctrl, 2 *Gfp*-SD, and 1 *Setd7*-SD) and 8 female samples (2 *Gfp*-Ctrl, 2 *Setd7*-Ctrl, 2 *Gfp*-SD, and 2 *Setd7*-SD). Male and female samples were combined for group-level analysis, such that each group comprised 3-4 samples. DESeq2 and edgeR tools were used to normalize read counts and perform differential gene expression (DEG) analysis. Genes with expression below -2.5 logCMP were filtered out. DEGs were defined as genes with an absolute log-fold change >0.58 (corresponding to a 50% fold-change) and uncorrected $p<0.01$ in order to evaluate pattern-level changes, as opposed to focusing on individual genes passing more stringent cutoffs.

Generation of a Setd7-over-expression viral vector

To directly test the hypothesis that elevated levels of H3K4me1 sensitized mice to future stress experience, we over-expressed the monomethyltransferase *Setd7* in developing VTA. In order to test this hypothesis, we first generated an adeno-associated virus carrying a *Gfp*- and Myc-tagged *Setd7* transgene (pAAV-EF1a-EGFP-P2A-Myc-Setd7-WPRE-hGHpA). cDNA for *Setd7* (#87131; originally gifted from Francesca Spagnoli; (Kofent et al., 2016)) and *Gfp* (pAAV-EF1a-EGFP-WPRE-hGHpA) were purchased from Addgene (#60058; originally gifted from Brandon Harvey; (Savolainen et al., 2014)). AAV-*Setd7* and AAV-*Gfp* control (identical, without *Myc-Setd7*) vectors were cloned and packaged by the Princeton Neuroscience Viral Core.

Western Blotting

To validate our viral construct's ability to increase SETD7 protein and the post-translational modification H3K4me1, and assess whether other related histone modifications were also altered by *Setd7* over-expression, we performed relative protein quantifications via Western blotting. A cohort of wild-type mice were injected with AAV-*Setd7* or AAV-*Gfp* in the VTA at P28. Fourteen days after surgery, 32 male mice were rapidly cervically dislocated, brains were removed immediately, placed into ice-cold PBS, and sliced into 1 mm-thick coronal sections in a brain matrix. Bilateral punches were made from VTA (16 gauge) and were homogenized on ice, in hypotonic lysis buffer (10 mM Tris, 1 mM KCl, 1.5 mM MgCl2, pH 8.0) supplemented with 1 mM Dithiothreitol (DTT), protease inhibitor cocktail (cOmplete™, EDTA-free, Millipore-Sigma) and histone deacetylase (HDAC) inhibitor (10 mM sodium butyrate). Samples were centrifuged for 10 minutes at 10,000xg at 4˚C to extract nuclei. Supernatants were discarded and pellets were resuspended in RIPA buffer (50 mM Tris, 150 mM sodium chloride, Triton X-100, 0,1% SDS, pH 8.0) supplemented with 10 mM DTT, protease inhibitor cocktail (cOmplete™, EDTA-free, Millipore-Sigma) and HDAC inhibitor (10 mM sodium butyrate). Protein concentration was evaluated with a 660nm Protein Assay (Pierce). Proteins were separated by SDS-PAGE gels (4-20%, BioRad) and transferred to 0.2 µm low-fluorescence PVDF membranes (Amersham Hybond). The following antibodies were used: H3 (1:5,000, ab24834, Abcam), H3K4me1 (1:2,000, ab8895, Abcam), H3K4me3 (1:1,000, ab8580, Abcam), H3K27ac (1:1,000, 07-360, Millipore-Sigma), SETD7(1:500, TA503322, Origene), and GAPDH (1:2,000, 2118, Cell Signaling). Secondary antibodies were Alexa Fluor 647 anti-rabbit (1:1,000, 711-605-152, Jackson ImmunoResearch) and AffinipureCy3 anti-mouse (1:1000, 715-165-150, Jackson ImmunoResearch). Images were acquired with Azure Imaging System (Azure Biosystems) and quantified using ImageJ.

Immunohistochemistry and imaging

A portion of the mice that received viral over-expression and underwent behavioral testing were used to assess targeting and specificity of viral expression. Mice were sacrificed a day after the last behavior testing. Mice were anesthetized with ketamine/xylazine (100 mg/kg and 10 mg/kg, i.p.) and transcardially perfused with sterile 1X PBS followed by 4% paraformaldehyde. Brains were removed, equilibrated in 30% sucrose in PBS, and frozen at -80˚C until processing. Brains were sectioned at 50 µm-thick slices using a cryostat. Immunohistochemistry was performed using the following antibodies: SETD7 (Origene, TA503322), GFP (Aves Lab, GFP-1020), and Prolong Gold Antifade with DAPI (Invitrogen). Imaging was performed on Hamamatsu NDP slide scanner (Hamamatsu Nanozoomer 2.0HT).

Statistical analysis for gene expression, protein quantification, and behavior

All statistics were performed using SPSS (Version 26) or Prism (GraphPad; version 9), with alpha set to 0.05. Outliers were defined as more than two standard-deviations away from group mean within cohort and were removed to avoid type-two error. Effects of early-life and adult stress were assessed using ANOVA or mixed-effects modeling, as indicated. Post-hoc analyses between pairs of groups were conducted using Tukey's multiple-comparisons correction if there were significant main effects or interactions. Significant changes in proportion of susceptible or resilient mice in the social avoidance task were calculated by two-tailed two-proportion z-test. All data are plotted as mean ± the standard error of the mean (SEM).

Data Availability

All relevant data that support the findings of this study are available by request from the corresponding author (CJP). RNA-sequencing data will be deposited with GEO.

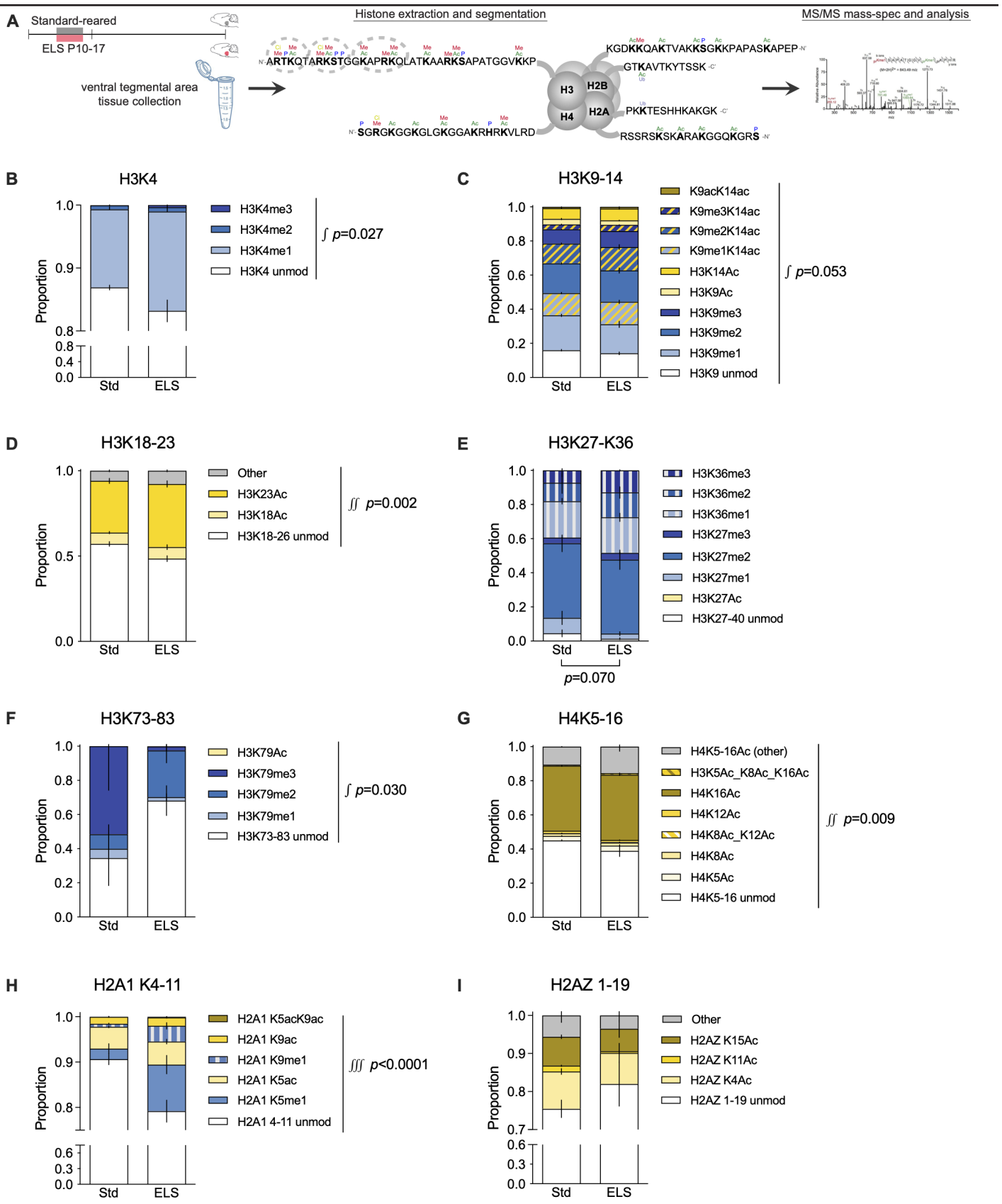

Figure 1: ELS alters proportions of histone modifications in VTA.
(A) Study design overview: Male mice were either standard-reared (Std) or experienced ELS from P10-17, followed by standard conditions until adulthood. VTA was extracted, histones purified and histone tails fragmented, and subjected to LC-MS/MS. **(B-I)** Proportions of PTHM's on each histone tail fragment for Std and ELS. Methylation is shown with blue shades, acetylation is shown with yellows, and dual modifications are shown with stripes. Vertical bars depict standard error from three pooled biological replicates each. Interactions between ELS and PTHM proportions are indicated by ∫ with the p-value shown; main effects of ELS are indicated below the bars.

RESULTS

ELS alters histone methylation and acetylation dynamics in the VTA

In order to quantify proportions of PTHMs in VTA and their changes following ELS, we used unbiased, label-free mass spectrometry (LC-MS/MS) in VTA from adult male standard-reared and ELS mice (**Figure 1A**). Such analyses allow for simultaneous quantification of hundreds of histone PTHM states within the same sample, both in isolation and combinatorially with adjacent post-translational modifications; co-occurring combinations of modifications within a fragment are possible when that fragment includes multiple possible peptides that can be methylated or acetylated. We identified a unique pattern of single and combinatorial states of methylation and acetylation occurring on histone H3, histone H4 and variant histone proteins H2A.1 and H2A.Z.1 following ELS relative to controls.

Of the 27 peptide fragments detected, there was a significant ($p<.05$) or trending ($p<0.1$) interaction between rearing condition and PTHM proportion within six peptide fragments (**Figure 1B-D, E-H**): **H3K3-8** [$F(3,12)=4.318$, $p=0.028$]; **H3K9-17** [$F(9,36)=2.123$, $p=0.053$, trend-level]; **H3K18-26** [$F(3,12)=9.432$, $p=0.002$]; **H3K73-83** [$F(4, 16)=3.520$, $p=0.030$]; **H4K5-16** [$F(7,28)=3.378$, $p=0.009$]; and **H2A1K4-11** [$F(5,20)=15.04$, $p<0.0001$]. We also detected a trend-level main effect of ELS within one histone fragment (**Figure 1E**): **H3K27-36** [$F(1,4)=6.00$, $p=0.070$]. Within these fragments, ELS increased proportions of four PTHMs/combinations including: H3K9me3 ($p=0.031$), H3K9me3-K14Ac ($p=0.031$), H3K23Ac ($p=0.044$), H3K36me2 ($p=0.034$), H4K8Ac ($p=0.019$), H4K8Ac-K12Ac ($p=0.011$), H4K5Ac-K8Ac-K16Ac ($p=0.024$), H2A.1K5me1 ($p=0.026$), and H2A.1K9me1 ($p=0.018$), and a trend for increased **H3K4me1** ($p=0.092$), H3K4me3 ($p=0.070$), H3K9Ac-K14Ac ($p=0.056$), and H2A.1K5Ac-K9Ac ($p=0.052$) (**Supplemental Figure 1**). ELS decreased proportions of unmodified H3K18-26 ($p=0.017$), unmodified H2A.1K4-11 ($p=0.013$), and H2AZK11Ac ($p=0.044$), with a trend for decreased H4K5Ac-K12Ac ($p=0.064$) (**Supplemental Figure 1**). Interestingly, a majority of these modifications are associated with open chromatin state and would predict active, primed or poised gene expression, such that ELS would be predicted to increase transcriptional potential or facilitate gene expression responses. These results indicate that ELS alters histone dynamics in VTA that endure into adulthood.

ELS alters the H3K4 monomethyltransferase Setd7

In order to determine whether changes in PTHMs could be driven by changes in corresponding histone-modifying enzymes, we first examined published gene expression data from adult male VTA after ELS and/or adult social defeat stress (GEO accession GSE89692; Peña et al., 2017), and next validated expression levels of several enzymes in an independent cohort including both male and female mice exposed to ELS and/or adult social defeat stress. Relative expression levels from published RNA-seq data were calculated as fold-change from standard-reared control group normalized expression. We examined expression of four H3K4 methyltransferases (*Kmt2a*, *Kmt2b*, *Kmt2c*, and *Setd7*), two lysine demethylases (*Kdm1a* and *Kdm1b*), two H3K9 methyltransferases (*Setdb1* and *Ehmt2*a also known as G9a), the H3K27 methyltransferase *Ezh2*, two histone acetyltransferases (*Crebbp* and *Ep300* also known as CBP/p300), and five histone deacetylases (*Hdac2*, *Hdca3*, *Hdac5*, *Hdac11*, and *Sirt1*). There was an interaction between ELS and social defeat on *Setd7* expression [$F(1,16)=7.389$,

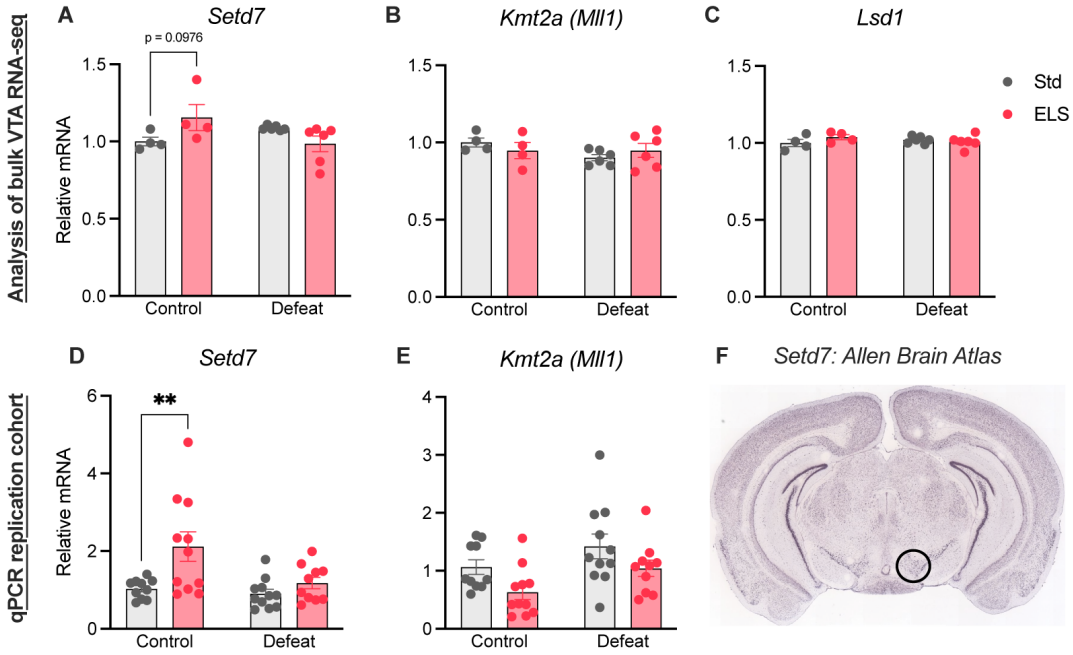

Figure 2: ELS alters expression of the H3K4 monomethyltransferase *Setd7*.
Relative changes in mRNA expression of known H3K4 methyltransferases **(A)** *Setd7*, **(B)** *Kmt2a*, and **(C)** the lysine demethylase *Lsd1* in published bulk RNA-sequencing data (GEO GSE89692) from the VTA of male mice that were standard- or ELS-reared and exposed to control or social defeat conditions in adulthood. Relative changes in mRNA by qPCR in a replication cohort of male and female mice for **(D)** *Setd7* and **(E)** *Kmt2a*. Data are represented as mean ± SEM with $^{**}p<0.01$. Allen Brain Atlas *in situ* hybridization showing **(F)** that *Setd7* is highly expressed in the dopaminergic VTA and substantia nigra at P56 (VTA is circled).

p=0.015] with a trend for ELS to increase *Setd7* expression relative to standard-reared control mice (post-hoc with sidak's multiple comparisons test p=0.098) (**Figure 2A**). There was no effect of ELS, social defeat, or their interaction for any other epigenetic enzyme examined (*Kmt2a* and *Lsd1* shown; **Figure 2B-C**).

Within a replication cohort including both males and females where gene expression was assessed by qPCR, we found a main effect of ELS on *Setd7* expression [F(1,38)=9.147, p=0.004], a main effect of social defeat [F(1,38)=5.672, p=0.022], and a trending interaction [F(1,38)=3.275, p=0.078] (**Figure 2D**). ELS specifically increased *Setd7* expression among control mice [post-hoc with sidak's multiple comparisons test p=0.003], but not socially defeated mice. In this cohort, there was a main effect of ELS to suppress the mixed-lineage leukemia (MLL)-type H3K4 methyltransferase *Kmt2a* (MLL1) [F(1,38)=6.559, p=0.015] and a main effect of social defeat to increase expression [F(1,38)=5.837, p=0.021], but no significant post-hoc comparisons (standard vs ELS control mice p=0.12) (**Figure 2E**). In support of a role for *Setd7* in VTA, there is high *Setd7* expression within the dopaminergic VTA and the nearby substantia nigra in the Allen Brain Atlas at P56 (**Figure 2F**; Allen Institute for Brain Science, 2004). Together, these findings support the view that the increase in H3K4 monomethylation in VTA observed by mass spec is attributable to increased expression of *Setd7*.

Setd7 over-expression in mice specifically increases H3K4me1

SETD7 is a methyltransferase that specifically catalyzes the monomethylation of H3K4, without further catalyzing di- and tri-methylation at H3K4, or methylation at other histone lysine residues (Wang et al., 2001; Keating and El-Osta, 2013). Given the interaction between ELS and H3K4 methylation state and increased expression of *Setd7* in VTA, we hypothesized that elevated H3Kme1 in VTA may facilitate the response to adult stress. In order to increase levels of H3K4me1 in VTA to test this hypothesis, we generated a *Setd7* over-expression vector (pAAV-EF1a-EGFP-P2A-Myc-Setd7-WPRE-hGHpA; **Figure 3A**) and packaged it into AAVs. To verify whether *Setd7* over-expression led to an increase in total H3K4me1, we bilaterally injected AAVs-*Setd7* or AAV-*Gfp* in VTA of male mice. Two weeks after injections, VTA tissue punches were harvested and processed and protein levels were quantified by Western blotting. We observed a 4-fold increase in total SETD7 compared to GFP-injected control mice, including SETD7 protein at native 40.1 kDA size and SETD7 that remained fused to Myc and GFP tags [t(22)=3.211, p=0.004; unpaired t-test; **Figure 3B**]. We also quantified the ability of *Setd7* over-expression to alter H3K4 methylation. *Setd7* over-expression successfully elevated H3K4me1 levels by 34% relative to GFP control, normalized to total H3, consistent with its role as a monomethyltransferase [t(22)=5.314, p<0.0001; **Figure 3C**]. However, there was no change in H3K4me3 or H3K27Ac [**Figure 3D-E**]. These results indicate that *Setd7* over-expression is able to specifically monomethylate H3K4 without recruiting further H3K4 methylation or other histone modifications associated with active gene expression.

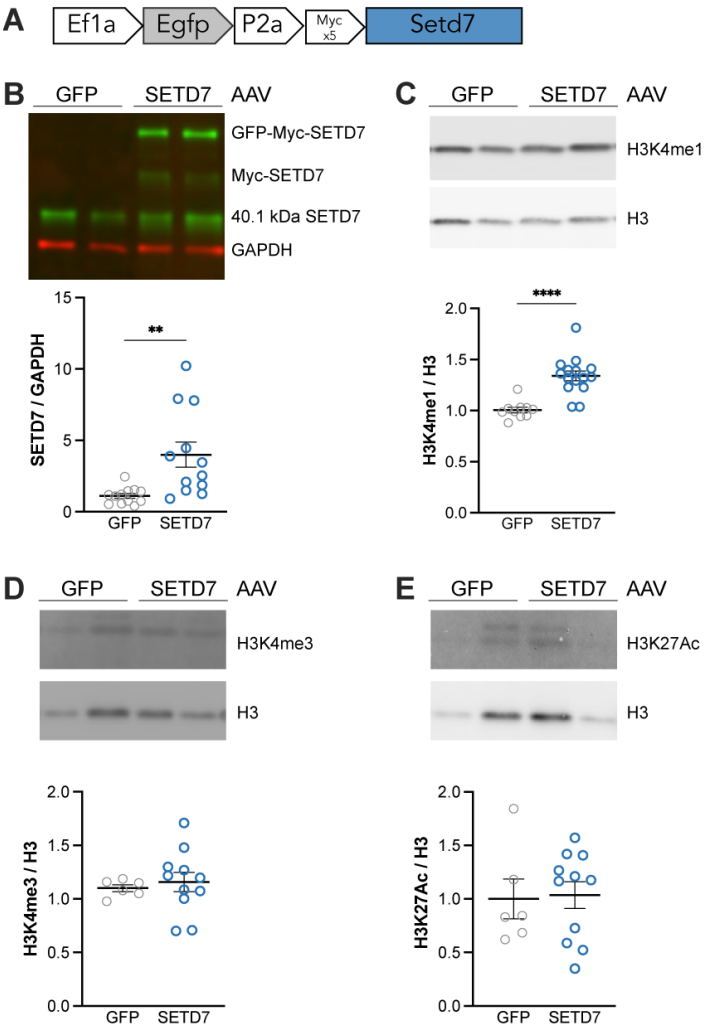

Figure 3: *Setd7* over-expression in VTA increases levels of SETD7 and H3K4me1 but not K4me3 or H3K27Ac.
(A) Viral vector design for over-expression of *Gfp-Myc-Setd7*. Bilateral AAV-*Setd7* injection into the VTA increases **(B)** total SETD7 protein and **(C)** H3K4me1 levels compared to AAV-*Gfp*-injected controls, while **(D)** H3K4me3 and **(E)** H3K27Ac levels remain unchanged. Example Western blots and for protein or post-translational modifications are shown with either GAPDH or total histone H3 loading controls. Data are represented as mean ± SEM with **p<0.01 and ****p<0.0001.

Setd7 over-expression in VTA enhances sensitivity to adult stress

To test the hypothesis that SETD7-driven H3K4me1 enrichment in VTA enhances stress sensitivity as a potential mechanism of ELS-driven stress sensitivity, we over-expressed AAV-*Setd7* or AAV-*Gfp* control in developing VTA at P14 of male and female mice, during the ELS sensitive period (Peña et al., 2017, 2019a), and evaluated behavioral

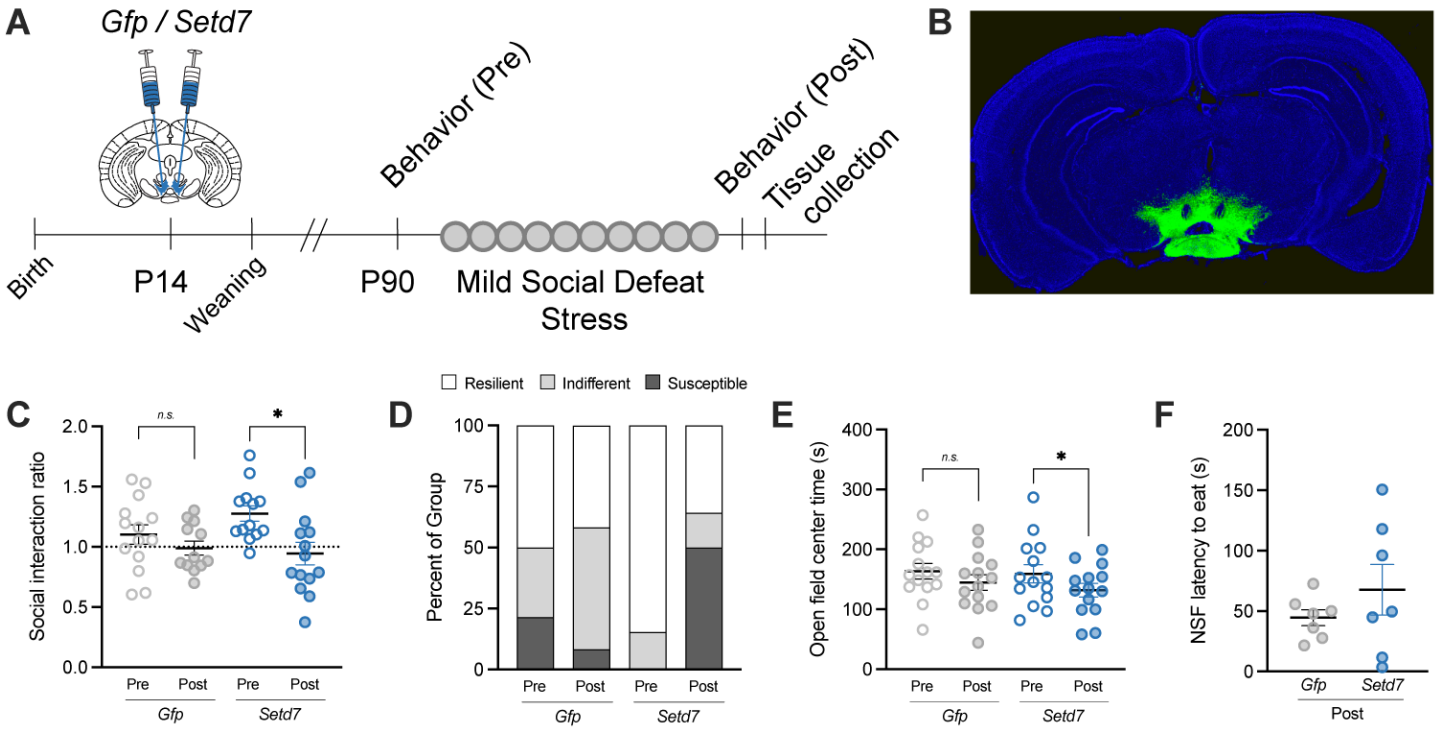

Figure 4: Juvenile *Setd7* over-expression enhances sensitivity to adult stress.
(A) Experimental design: AAV-*Setd7* or AAV-*Gfp* was bilaterally injected into VTA of male and female mice at P14. Behavior was quantified before (pre) and after (post) mild social defeat stress. **(B)** GFP confirmation of the spatial accuracy of juvenile AAV injections. **(C)** Social interaction ratio (time spent investigating a novel aggressive mouse vs empty enclosure) was reduced by mild social defeat among AAV-*Setd7* (p=0.0036) but not AAV-*Gfp* mice. **(D)** AAV-*Setd7*, but not AAV-*Gfp* increased the proportion of mice behaviorally categorized as susceptible to mild social defeat stress. **(E)** Time spent in the center of an open field was reduced by mild social defeat among AAV-*Setd7* (p=0.049) but not AAV-*Gfp* mice. **(F)** AAV-*Setd7* injection does not significantly increase novelty-suppressed feeding latency in female mice following mild social defeat stress.

and gene expression responses to adult social defeat stress (**Figure 4A**). A "non-discriminatory" variant of adult social defeat was used that was previously found to be an effective stressor in both male and female mice (Yohn et al., 2019). However, aggressor mice in these experiments were observed to attack less overall with females present, and thus defeat was considered mild for these experiments compared to the standard ten days of male-only social defeat stress (e.g. Peña et al., 2017). For behavioral testing, we used a within-subject test design to assess mice for social and exploratory avoidance behaviors before ("pre") and after ("post") social defeat stress. We also confirmed that our viral targeting of developing VTA was successful and relatively specific (**Figure 4B**). This was a particular challenge, given the young age of pups during surgery and deep-brain location of the VTA. There was a main effect of social defeat on social interaction ratio [mixed-effects model: $F(1,49)=8.240$, p=0.0060; interaction between *Setd7* and defeat p=0.163]. Post-hoc testing revealed that there was an effect of defeat only within *Setd7* mice [Fisher's LSD for *Setd7* (p=0.0036) vs. *Gfp* (p=0.313); **Figure 4C**]. There was no effect of sex. Among *Setd7* but not *Gfp* mice, defeat increased the proportion considered susceptible (Z=2.96, p=0.003; **Figure 4D**) and decreased the proportion considered resilient (Z=2.58, p=0.010). Similarly, within an open field test, there was a main effect of social defeat on center time [two-way ANOVA with paired effects: $F(1,26)=6.017$, p=0.0212; **Figure 4E**] such that defeat decreased center time among *Setd7* mice (p=0.049) but not *Gfp* mice (p=0.178). We also ran a novelty-suppressed feeding test in female mice after social defeat (following earlier findings that this test was sensitive among female ELS mice from Peña et al., 2019b; Parel et al., 2023 but did not find an effect of *Setd7* on latency to eat (**Figure 4F**). Together, these results indicate that developmental *Setd7* over-expression increases sensitivity to mild adult social defeat stress among both male and female mice.

Setd7 over-expression during early life augments transcriptional responses to adult stress

We next tested that the enhanced stress sensitivity seen upon developmentally increasing H3K4me1 in VTA via *Setd7* over-expression is associated with enhanced transcriptional reactivity, as gene expression constitutes a direct readout of the epigenome. We generated a second cohort of mice with juvenile (P14) *Setd7* or *Gfp* over-expression that included distinct control and adult social defeat groups and performed bulk-tissue RNA-sequencing on VTA. As deposition of H3K4me1 by *Setd7* over-expression was assumed to be broad across the genome, we focused on pattern-level changes (setting differential expression criteria at p<0.01 and fold-change greater than

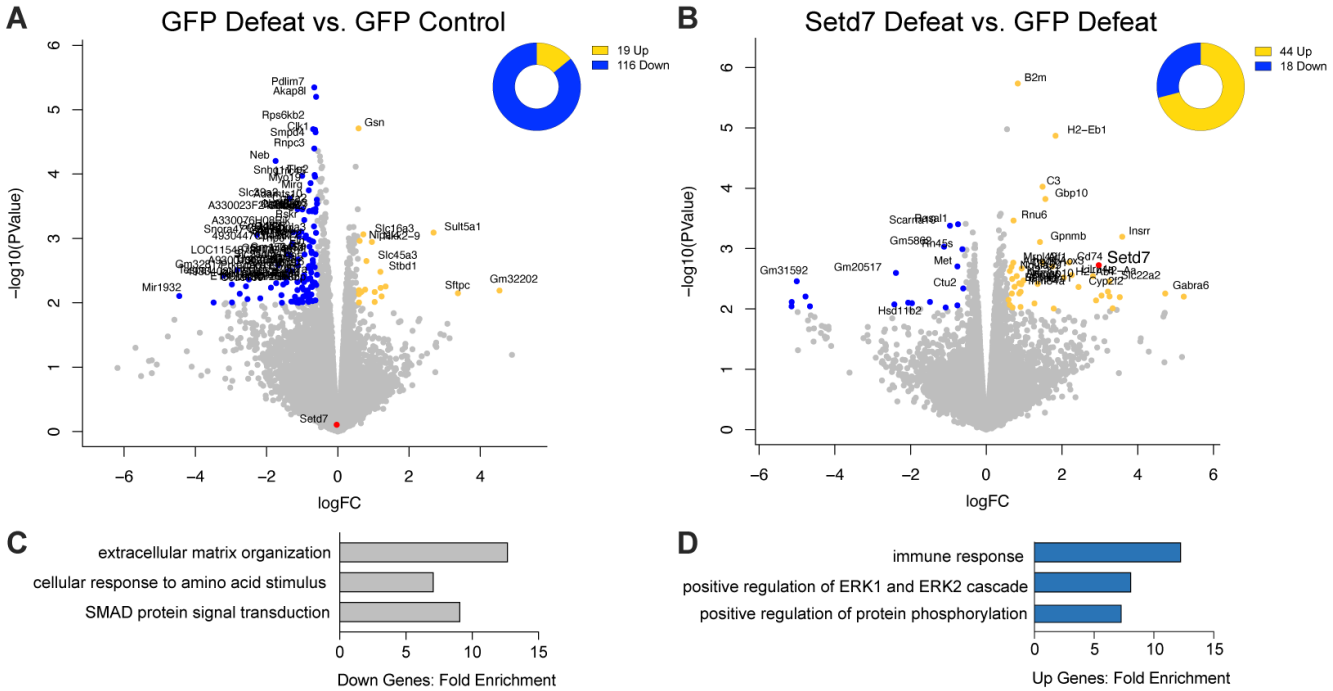

Figure 5: Juvenile *Setd7* over-expression augments transcriptional responses to adult stress.
(A) Volcano plot of differentially expressed genes (DEGs) in VTA among AAV-*Gfp* mice subjected to mild social defeat stress compared to control conditions, demonstrating 86% of DEGs are downregulated. **(B)** Gene ontology enrichment analysis of DEGs downregulated by GFP-Defeat vs GFP-Control. **(C)** Volcano plot of DEGs in VTA between stressed AAV-*Setd7* stressed mice compared to stressed AAV-*Gfp* mice, demonstrating that 73% of DEGs were upregulated. **(D)** Gene ontology enrichment analysis of DEGs upregulated by Setd7-Defeat vs GFP-Defeat.

50%) rather than individual genes. We first examined the impact of social defeat stress on gene expression within *Gfp* control mice and found that defeat stress predominantly decreased gene expression, with 116 genes down-regulated and only 19 genes up-regulated by these criteria (**Figure 5A**). This pattern of largely suppressed gene expression is consistent with previous findings that approximately 70% of genes altered by adult stress were down-regulated in VTA (Peña et al., 2019b). Genes down-regulated by defeat stress among *Gfp* control mice were enriched for functions related to extracellular matrix organization, cellular response to amino acid stimulus and SMAD signal transduction (**Figure 5B**). We then examined the impact of defeat stress on gene expression among mice epigenetically primed by *Setd7* vs *Gfp* and found that *Setd7* predominately increased gene expression responses to defeat, with 44 genes up-regulated (71%; **Figure 5C**) and only 18 down-regulated. As expected, *Setd7* was among the top most enriched genes (**Figure 5C**). Genes up-regulated by *Setd7* over-expression and defeat were enriched for functions related to immune response, ERK cascade regulation, and protein phosphorylation (**Figure 5D**). Notably, down-regulated genes included *Hsd11b2* (encoding the enzyme that inactivates glucocorticoids by oxidizing corticosterone into its inactive metabolite; Seckl et al., 2002), which would lead to prolonged glucocorticoid signaling and stress hypersensitivity (Jensen Peña et al., 2012). These findings indicate that epigenetic priming within VTA by over-expression of *Setd7* increases transcriptional reactivity to adult stress.

DISCUSSION

ELS increases sensitivity to subsequent stress, which has been observed among humans (McLaughlin et al., 2010; Saxton and Chyu, 2019; Sidamon-Eristoff et al., 2022) and animal models (Howell et al., 2014; Zhang et al., 2016; Peña et al., 2017, 2019a) at the level of behavior, cellular activity (Balouek et al., 2023), and gene expression (Peña et al., 2019b; Kos et al., 2023). We tested the hypothesis that persistent changes in transcription and transcriptional potential in VTA were maintained at the level of the epigenome, through changes in chromatin. Here, using a combination of bottom-up mass spectrometry, viral-mediated epigenome-editing, behavioral quantification, and RNA-sequencing, we show that ELS alters histone dynamics in the VTA and that mimicking one such prominently altered histone modification recapitulates ELS-induced behavioral and transcriptional hypersensitivity to future stress in adulthood.

ELS triggered enduring changes among a variety of histone methylation and acetylation modifications in VTA, across histones H3, H2A, and H4 (**Figure 1**; **Supplemental Figure 1**). Interestingly, 75% of histone modification changes were associated with a permissive (open, active, primed, or poised) state, among modifications with at least trending individual significance and known relationship with transcription. This broad finding suggests that ELS may facilitate transcriptional response to future stress via a more

permissive, or "primed," chromatin state, although a direct quantification of chromatin accessibility in VTA following ELS is needed. These findings are consistent with broad and dynamic histone modifications reported following ELS in NAc, a direct target of VTA dopamine neurons, including an increase in H3K4me1 in adolescent males and females and adult males (Kronman et al., 2021). Across histone 3 modifications often associated with gene repression, we found that ELS increases both H3K9me3 and H3K36me2. Recently, the co-occurrence of H3K9 and H3K36 methylation has been hypothesized to 'bookmark' enhancers for future transcriptional activity during embryonic stem cell differentiation (Barral et al., 2022), although it is not yet known whether the dual-occurrence of these marks functions similarly in the postnatal brain.

These mass-spec data also support an emerging role for histone variant incorporation and turnover in facilitating the transcriptional response to ELS in the VTA. We observed that levels of H2A.Z, a replication-independent histone H2A variant which is involved in heterochromatin formation and transcriptional control (Giaimo et al., 2019), is modified following ELS. H2A.Z-K11Ac is lower the adult VTA after ELS, potentially indicating lower overall levels of active transcription. Conversely, H3K4me1 and H3K4me3 (increased following ELS) are recognized by "reader" subunits of an H2A.Z loading complex and have been shown to facilitate later H2A.Z loading (Giaimo et al., 2019). H2A.Z loading and transcriptional activation are also dependent upon H4 and H2A acetylation, which are likewise elevated in adult VTA after ELS in the current study (H4K8Ac, H4K8Ac-K12Ac, H4K5Ac-K8Ac-K16Ac; H2A.1K5Ac-K9Ac). This finding is consistent with the idea that ELS may prime chromatin for future transcriptional reactivity, but does not cause constitutively active transcription. However, our results reported here do not distinguish between changes in endogenous histone variant post-translational modifications, or changes in the incorporation of variants into nucleosomes which are subsequently post-translationally modified. Thus, it is unclear if global changes in H2A.Z variant abundance reflect modifications to extant loci harboring H2A.Z, or a shift in abundance through variant incorporation at other loci, or a combination of both. Similarly, ELS was previously found to increase levels of H3.3 — the predominant form of H3 in adult neurons — in NAc across development, associated with regulation of activity-dependent neuronal transcription, synaptic connectivity, and behavioral plasticity (Lepack et al., 2016), together indicating that ELS causes enduring epigenetic reprogramming across reward circuitry as a potential mechanism for increased behavioral sensitivity to stress.

Importantly, our mass spectrometry data from ELS-treated mice broadly agrees with prior investigations of the reward-associated dynamics of specific PTHMs in the VTA. Within VTA, previous work found that a single 24-hour period of maternal separation on postnatal day P9 (similar to our findings of a sensitive period for ELS starting in the second postnatal week; Peña et al., 2017) decreased H3K9Ac (Shepard et al., 2018). Adolescent ethanol exposure also reduces global levels of VTA H3K9ac abundance, and leads to putative dopamine neuron hyposensitivity to exogenous GABA inhibition (Arora et al., 2013; Shepard and Nugent, 2020). Consistent with this earlier work, we also see reduced levels of H3K9Ac in VTA after ELS, although this change did not reach significance in our mass-spec data with only three biological replicates. Interestingly, changes in VTA H3K9Ac were associated with impaired GABAergic synaptic plasticity and increased long-term depression of GABAergic neurons onto dopamine neurons, resulting in metaplasticity and increased dopamine neuron excitability and release (Authement et al., 2015; Shepard et al., 2018, 2020). Together, these findings indicate consistent and functional relevance of ELS-induced chromatin modifications in VTA, linking molecular changes with neuronal activity and behavior, as well as the need for cell-type specificity in future studies.

Despite changes among a variety of histone modifications in VTA, we found few enduring changes in the enzymes that write and erase these modifications. In fact, the only consistently altered histone-modifying enzyme across two cohorts of mice was *Setd7* (**Figure 2A-E**). SETD7 (SET7/9, KMT7) is a histone lysine methyltransferase that deposits a single methyl group at H3K4, often at gene promoters (Wang et al., 2001; Kwon et al., 2003; Xiao et al., 2003; Calo and Wysocka, 2013; Keating and El-Osta, 2013). Its role as a specific monomethyltransferase is unique relative to better-known H3K4 methyltransferases including KMT2A, KMT2B, KMT2C, KMT2D, KMT2E, and KMT2F (MLL1, MLL2, MLL3, MLL4, SET1A, and SET1B, respectively) that are capable of serially adding di- and tri-methylation to H3K4, and in some cases have higher substrate specificity for methylated H3K4 (Del Rizzo and Trievel, 2011; Collins et al., 2019). Methylation by SETD7 also plays an emerging role in the stability and subcellular localization of non-histone proteins, the downstream effects of which can both promote or suppress transcription in a context-dependent manner (Keating and El-Osta, 2013; Batista and Helguero, 2018; Chiang et al., 2022). While we cannot currently rule out effects based on potential non-histone substrates, both the increase in SETD7 in nuclear protein lysates and the increase in H3K4me1 indicate that this is at least a prominent, if not exclusive, function. The ability of *Setd7* over-expression to increase H3K4me1 but not H3K4me3 in our experiments (**Figure 3C-E**) corroborates its role as a selective monomethyltransferase. H3K4me1 and H3K4me3 have distinct enrichment across the genome, with H4K3me1 marking both active promoters and enhancers and poised/primed regulatory regions, while H3K4me3

is highly enriched at active promoter regions (Calo and Wysocka, 2013). These distinct distribution patterns require distinct regulation themselves and serve distinct functions, suggesting specificity in the impact of ELS on genomic regulation. *Setd7* also showed interesting specificity in its expression pattern in the brain with enrichment in the VTA and substantia nigra relative to surrounding regions (**Figure 2F**), potentially suggesting functional specificity for dopaminergic modulation.

Consistent with a role for H3K4me1 to "prime" transcriptional responses, we found that early developmental (P14) over-expression of *Setd7* in VTA increases transcriptional and behavioral responses to adult stress (**Figures 4-5**). These findings demonstrate that *Setd7* over-expression in the VTA is sufficient to recapitulate the effect of ELS to increase behavioral stress susceptibility. The increase in upregulated genes after social defeat with AAV-*Setd7* was notable in contrast to largely decreased VTA transcription in AAV-*Gfp* mice. This decrease in transcription with social defeat is consistent with earlier work which also reported largely decreased transcription after adult stress in VTA (Peña et al., 2019b). However, we are cautious to put too much emphasis on individual genes altered by *Setd7* over-expression here given that this AAV over-expression vector is a blunt tool and we do not have control over where H3K4me1 is deposited across the genome. It is likely to be deposited in genomic regions that are already open and accessible to the enzyme. This begs the need for future research with more refined tools such as CRISPR/Cas9-based targeted epigenetic modifications for improved specificity (Pulecio et al., 2017; Savell et al., 2019; Lorsch et al., 2019). Nevertheless, together, these findings are consistent with the hypothesis that SETD7-driven H3K4me1 enrichment in VTA enhances stress sensitivity as a potential mechanism of ELS-driven stress sensitivity.

One lingering question in the context of our findings is a hypothesized role for H3K4me1 in affecting sensitivity to *positive*, as well as negative, valence stimuli. If chromatin priming of the VTA with *Setd7* and H3K4me1 drives susceptibility to aversive experiences in adulthood, it remains possible that the VTA could equally become hyper-responsive to nonstressful environmental conditions, such as environmental enrichment. Similar populations of VTA dopamine neurons have been shown to encode a variety of distinct stimuli, including both unexpected aversive and unexpected rewarding experiences (Del Arco et al., 2020; Willmore et al., 2023). The potential for epigenetic priming to drive sensitivity to positive, enriching experiences would open new possible avenues for intervention for individuals who have experienced childhood adversity.

In conclusion, enduring changes in histone modifications suggest that ELS promotes a more open/permissive chromatin state in the VTA, known to facilitate responses to future stimuli. Mimicking increases in the monomethyltransferase *Setd7* and H3K4me1 recapitulates ELS-induced behavioral and transcriptional hypersensitivity to future stress. Together these findings point to a role for epigenetic priming as a possible biological mechanism through which ELS programs later stress sensitivity.

ACKNOWLEDGEMENTS

This research was funded by NIH R00MH115096 (CJP); NIH R01MH129643 (CJP); R01MH116900 (IM); Howard Hughes Medical Institute (IM); NIH R01MH129306 (EJN); NIH R01NS111997 (BAG); NIH R01HD106051 (BAG); New York Stem Cell Foundation (CJP). CJP is a New York Stem Cell Foundation Robertson Investigator and Robin Chemers Neustein Fellow. We would like to thank Natarajan Bhanu for her work processing mass-spec samples, Esteban Engel and the Princeton Neuroscience Viral Core for assistance generating the AAV-*Setd7* over-expression vector, and Wei Wang and the Genomics Core Facility in the Lewis-Sigler Institute for Integrative Genomics at Princeton where RNA-seq was performed. Parts of some figures were generated with BioRender.com.

AUTHOR CONTRIBUTIONS

The histone modification studies were designed by CJP and IM. The SETD7 studies were designed by JAB and CJP. Histone modification data were collected by CJP and LAF in the labs of EJN, IM, and BAG. SETD7 animal work was performed by JAB, LTG, and SNB. SEDT7 molecular data were collected by JAB and LTG. Bioinformatic analysis was performed by ASC, MT, and CJP. All data were analyzed and figures generated by CJP, JAB, and LTG. The manuscript was written by LTG, JAB, and CJP with input from all authors.

COMPETING INTERESTS

There are no conflicts of interest to report.

REFERENCES

Allen Institute for Brain Science (2004). Allen Mouse Brain Atlas. Available at: http://mouse.brain-map.org/experiment/show?id=71016630

Arora, D. S., Nimitvilai, S., Teppen, T. L., McElvain, M. A., Sakharkar, A. J., You, C., et al. (2013). Hyposensitivity to Gamma-Aminobutyric Acid in the Ventral Tegmental Area During Alcohol Withdrawal: Reversal by Histone Deacetylase Inhibitors. *Neuropsychopharmacology* 38, 1674–1684. doi: 10.1038/npp.2013.65

Authement, M. E., Kodangattil, J. N., Gouty, S., Rusnak, M., Symes, A. J., Cox, B. M., et al. (2015). Histone Deacetylase Inhibition Rescues Maternal Deprivation-Induced GABAergic Metaplasticity through Restoration of AKAP Signaling. *Neuron* 86, 1240–1252. doi: 10.1016/j.neuron.2015.05.024

Balouek, J.-A., Mclain, C. A., Minerva, A. R., Rashford, R. L., Bennett, S. N., Rogers, F. D., et al. (2023). Reactivation of Early-Life Stress-Sensitive Neuronal Ensembles Contributes to Lifelong Stress Hypersensitivity. *J. Neurosci.* 43, 5996–6009. doi: 10.1523/JNEUROSCI.0016-23.2023

Barral, A., Pozo, G., Ducrot, L., Papadopoulos, G. L., Sauzet, S., Oldfield, A. J., et al. (2022). SETDB1/NSD-dependent H3K9me3/H3K36me3 dual heterochromatin maintains gene expression profiles by bookmarking poised enhancers. *Molecular Cell* 82, 816-832.e12. doi: 10.1016/j.molcel.2021.12.037

Bastle, R. M., and Maze, I. (2019). Chromatin Regulation in Complex Brain Disorders. *Current opinion in behavioral sciences* 25, 57–65. doi: 10.1016/j.cobeha.2018.07.004

Batista, I. de A. A., and Helguero, L. A. (2018). Biological processes and signal transduction pathways regulated by the protein methyltransferase SETD7 and their significance in cancer. *Sig Transduct Target Ther* 3, 1–14. doi: 10.1038/s41392-018-0017-6

Bennett, S. N., Chang, A. B., Rogers, F. D., Jones, P., and Peña, C. J. (2024). Thyroid hormones mediate the impact of early-life stress on ventral tegmental area gene expression and behavior. *Hormones and Behavior* 159, 105472. doi: 10.1016/j.yhbeh.2023.105472

Berton, O., Mcclung, C. A., Dileone, R. J., Krishnan, V., Renthal, W., Russo, S. J., et al. (2006). Essential role of BDNF in the mesolimbic dopamine pathway in social defeat stress. *Science* 311, 864–868. doi: 10.1126/science.1120972

Bhanu, N. V., Sidoli, S., and Garcia, B. A. (2020). A Workflow for Ultra-rapid Analysis of Histone Post-translational Modifications with Direct-injection Mass Spectrometry. *Bio Protoc* 10, e3756. doi: 10.21769/BioProtoc.3756

Bodnoff, S. R., Suranyi-Cadotte, B., Quirion, R., and Meaney, M. J. (1989). A comparison of the effects of diazepam versus several typical and atypical anti-depressant drugs in an animal model of anxiety. *Psychopharmacology* 97, 277–279. doi: 10.1007/BF00442264.pdf

Brake, W. G., Zhang, T. Y., Diorio, J., Meaney, M. J., and Gratton, A. (2004). Influence of early postnatal rearing conditions on mesocorticolimbic dopamine and behavioural responses to psychostimulants and stressors in adult rats. *European Journal of Neuroscience* 19, 1863–1874. doi: 10.1111/j.1460-9568.2004.03286.x

Cabib, S., Puglisi-Allegra, S., and D'amato, F. R. (1993). Effects of postnatal stress on dopamine mesolimbic system responses to aversive experiences in adult life. *Brain Research* 604, 232–239. doi: 10.1016/0006-8993(93)90374-V

Calo, E., and Wysocka, J. (2013). Modification of Enhancer Chromatin: What, How, and Why? *Molecular Cell* 49, 825–837. doi: 10.1016/j.molcel.2013.01.038

Chiang, C., Yang, H., Zhu, L., Chen, C., and Zheng, D. (2022). The Epigenetic Regulation of Nonhistone Proteins by SETD7: New Targets in Cancer. *Front. Genet.* 13. doi: 10.3389/fgene.2022.918509

Collins, B. E., Greer, C. B., Coleman, B. C., and Sweatt, J. D. (2019). Histone H3 lysine K4 methylation and its role in learning and memory. *Epigenetics & Chromatin* 12, 7. doi: 10.1186/s13072-018-0251-8

Covington, H. E., Maze, I., Sun, H., Bomze, H. M., DeMaio, K. D., Wu, E. Y., et al. (2011). A role for repressive histone methylation in cocaine-induced vulnerability to stress. *Neuron* 71, 656–670. doi: 10.1016/j.neuron.2011.06.007

Del Arco, A., Park, J., and Moghaddam, B. (2020). Unanticipated stressful and rewarding experiences engage the same prefrontal cortex and ventral tegmental area neuronal populations. *eNeuro*, ENEURO.0029-20.2020. doi: 10.1523/ENEURO.0029-20.2020

Del Rizzo, P. A., and Trievel, R. C. (2011). Substrate and product specificities of SET domain methyltransferases. *Epigenetics* 6, 1059–1067. doi: 10.4161/epi.6.9.16069

D'Urso, A., and Brickner, J. H. (2017). Epigenetic transcriptional memory. *Curr Genet* 63, 435–439. doi: 10.1007/s00294-016-0661-8

Farrelly, L. A., Thompson, R. E., Zhao, S., Lepack, A. E., Lyu, Y., Bhanu, N. V., et al. (2019). Histone serotonylation is a permissive modification that enhances TFIID binding to H3K4me3. *Nature* 128, 1. doi: 10.1038/s41586-019-1024-7

Giaimo, B. D., Ferrante, F., Herchenröther, A., Hake, S. B., and Borggrefe, T. (2019). The histone variant H2A.Z in gene regulation. *Epigenetics & Chromatin* 12, 37. doi: 10.1186/s13072-019-0274-9

Green, J. G., McLaughlin, K. A., Berglund, P. A., Gruber, M. J., Sampson, N. A., Zaslavsky, A. M., et al. (2010). Childhood Adversities and Adult Psychiatric Disorders in the National Comorbidity Survey Replication I. *Archives of general psychiatry* 67, 113–123.

Hanson, J. L., Albert, D., Iselin, A.-M. R., Carré, J. M., Dodge, K. A., and Hariri, A. R. (2016). Cumulative stress in childhood is associated with blunted reward-related brain activity in adulthood. *Social cognitive and affective neuroscience* 11, 405–412. doi: 10.1093/scan/nsv124

Hanson, J. L., Hariri, A. R., and Williamson, D. E. (2015). Blunted Ventral Striatum Development in Adolescence Reflects Emotional Neglect and Predicts Depressive Symptoms. *BPS* 78, 598–605. doi: 10.1016/j.biopsych.2015.05.010

Hanson, J. L., Williams, A. V., Bangasser, D. A., and Peña, C. J. (2021). Impact of Early Life Stress on Reward Circuit Function and Regulation. *Frontiers in Psychiatry* 12, 1799. doi: 10.3389/fpsyt.2021.744690

Heller, E. A., Cates, H. M., Peña, C. J., Sun, H., Shao, N., Feng, J., et al. (2014). Locus-specific epigenetic remodeling controls addiction- and depression-related behaviors. *Nature Neuroscience* 17, 1720–1727. doi: 10.1038/nn.3871

Hodes, G. E., Pfau, M. L., Purushothaman, I., Ahn, H. F., Golden, S. A., Christoffel, D. J., et al. (2015). Sex Differences in Nucleus Accumbens Transcriptome Profiles Associated with Susceptibility versus Resilience to Subchronic Variable Stress. *Journal of Neuroscience* 35, 16362–16376. doi: 10.1523/JNEUROSCI.1392-15.2015

Howell, B. R., Grand, A. P., McCormack, K. M., Shi, Y., LaPrarie, J. L., Maestripieri, D., et al. (2014). Early adverse experience increases emotional reactivity in juvenile rhesus macaques: Relation to amygdala volume. *Developmental Psychobiology* 56, 1735–1746. doi: 10.1002/dev.21237

Howerton, C. L., Morgan, C. P., Fischer, D. B., and Bale, T. L. (2013). O-GlcNAc transferase (OGT) as a placental biomarker of maternal stress and reprogramming of CNS gene transcription in development. *Proceedings of the National Academy of Sciences* 110, 5169–5174. doi: 10.1073/pnas.1300065110

Jensen Peña, C., Monk, C., and Champagne, F. A. (2012). Epigenetic effects of prenatal stress on 11β-hydroxysteroid dehydrogenase-2 in the placenta and fetal brain. *PLoS ONE* 7, e39791. doi: 10.1371/journal.pone.0039791

Jenuwein, T., and Allis, C. D. (2001). Translating the histone code. *Science* 293, 1074–1080. doi: 10.1126/science.1063127

Joseph, F. M., and Young, N. L. (2023). Histone variant-specific post-translational modifications. *Seminars in Cell & Developmental Biology* 135, 73–84. doi: 10.1016/j.semcdb.2022.02.012

Keating, S., and El-Osta, A. (2013). Transcriptional regulation by the Set7 lysine methyltransferase. *Epigenetics* 8, 361–372. doi: 10.4161/epi.24234

Kendler, K. S., Eaves, L. J., Loken, E. K., Pedersen, N. L., Middeldorp, C. M., Reynolds, C., et al. (2011). The impact of environmental experiences on symptoms of anxiety and depression across the life span. *Psychological Science* 22, 1343–1352. doi: 10.1177/0956797611417255

Kofent, J., Zhang, J., and Spagnoli, F. M. (2016). The histone methyltransferase Setd7 promotes pancreatic progenitor identity. *Development* 143, 3573–3581. doi: 10.1242/dev.136226

Kos, A., Lopez, J. P., Bordes, J., de Donno, C., Dine, J., Brivio, E., et al. (2023). Early life adversity shapes social subordination and cell type–specific transcriptomic patterning in the ventral hippocampus. *Science Advances* 9, eadj3793. doi: 10.1126/sciadv.adj3793

Krishnan, V., Han, M.-H., Graham, D. L., Berton, O., Renthal, W., Russo, S. J., et al. (2007). Molecular Adaptations Underlying Susceptibility and Resistance to Social Defeat in Brain Reward Regions. *Cell* 131, 391–404. doi: 10.1016/j.cell.2007.09.018

Kronman, H., Torres-Berrío, A., Sidoli, S., Issler, O., Godino, A., Ramakrishnan, A., et al. (2021). Long-term behavioral and cell-type-specific molecular effects of early life stress are mediated by H3K79me2 dynamics in medium spiny neurons. *Nature Neuroscience*, 1–10. doi: 10.1038/s41593-021-00814-8

Kwon, T., Chang, J. H., Kwak, E., Lee, C. W., Joachimiak, A., Kim, Y. C., et al. (2003). Mechanism of histone lysine methyl transfer revealed by the structure of SET7/9—AdoMet. *The EMBO journal* 22, 292–303. doi: 10.1093/emboj/cdg025

Lämke, J., and Bäurle, I. (2017). Epigenetic and chromatin-based mechanisms in environmental stress adaptation and stress memory in plants. *Genome Biology* 18, 124. doi: 10.1186/s13059-017-1263-6

Lepack, A. E., Bagot, R. C., Peña, C. J., Loh, Y.-H. E., Farrelly, L. A., Lu, Y., et al. (2016). Aberrant H3.3 dynamics in NAc promote vulnerability to depressive-like behavior. *Proc Natl Acad Sci USA* 113, 12562–12567. doi: 10.1073/pnas.1608270113

Lepack, A. E., Werner, C. T., Stewart, A. F., Fulton, S. L., Zhong, P., Farrelly, L. A., et al. (2020). Dopaminylation of histone H3 in ventral tegmental area regulates cocaine seeking. *Science* 368, 197–201. doi: 10.1126/science.aaw8806

Levine, A., Worrell, T. R., Zimnisky, R., and Schmauss, C. (2012). Early life stress triggers sustained changes in histone deacetylase expression and histone H4 modifications that alter responsiveness to adolescent antidepressant treatment. *Neurobiology of disease* 45, 488–498. doi: 10.1016/j.nbd.2011.09.005

Livak, K. J., and Schmittgen, T. D. (2001). Analysis of relative gene expression data using real-time quantitative PCR and the 2(-Delta Delta C(T)) Method. *Methods* 25, 402–408. doi: 10.1006/meth.2001.1262

Lorsch, Z. S., Hamilton, P. J., Ramakrishnan, A., Parise, E. M., Salery, M., Wright, W. J., et al. (2019). Stress resilience is promoted by a Zfp189-driven transcriptional network in prefrontal cortex. Nat Neurosci 22, 1413–1423. doi: 10.1038/s41593-019-0462-8

Marrocco, J., Gray, J. D., Kogan, J. F., Einhorn, N. R., O'Cinneide, E. M., Rubin, T. G., et al. (2019). Early Life Stress Restricts Translational Reactivity in CA3 Neurons Associated With Altered Stress Responses in Adulthood. *Frontiers in Behavioral Neuroscience* 13, 321. doi: 10.3389/fnbeh.2019.00157

Marusak, H. A., Hatfield, J. R. B., Thomason, M. E., and Rabinak, C. A. (2017). Reduced Ventral Tegmental Area-Hippocampal Connectivity in Children and Adolescents Exposed to Early Threat. *Biological psychiatry. Cognitive neuroscience and neuroimaging* 2, 130–137. doi: 10.1016/j.bpsc.2016.11.002

McLaughlin, K. A., Conron, K. J., Koenen, K. C., and Gilman, S. E. (2010). Childhood adversity, adult stressful life events, and risk of past-year psychiatric disorder: a test of the stress sensitization hypothesis in a population-based sample of adults. *Psychological medicine* 40, 1647–1658. doi: 10.1017/S0033291709992121

Morrison, K. E., Cole, A. B., Kane, P. J., Meadows, V. E., Thompson, S. M., and Bale, T. L. (2020). Pubertal adversity alters chromatin dynamics and stress circuitry in the pregnant brain. *Neuropsychopharmacology* 69, 1–9. doi: 10.1038/s41386-020-0634-y

Muir, J., Tse, Y. C., Iyer, E. S., Biris, J., Cvetkovska, V., Lopez, J., et al. (2020). Ventral Hippocampal Afferents to Nucleus Accumbens Encode Both Latent Vulnerability and Stress-Induced Susceptibility. *Biological Psychiatry* 0. doi: 10.1016/j.biopsych.2020.05.021

Parel, S. T., Bennett, S. N., Cheng, C. J., Timmermans, O. C., Fiori, L. M., Turecki, G., et al. (2023). Transcriptional signatures of early-life stress and antidepressant treatment efficacy. *Proceedings of the National Academy of Sciences* 120, e2305776120. doi: 10.1073/pnas.2305776120

Park, A. T., Tooley, U. A., Leonard, J. A., Boroshok, A. L., McDermott, C. L., Tisdall, M. D., et al. (2021). Early childhood stress is associated with blunted development of ventral tegmental area functional connectivity. *Developmental Cognitive Neuroscience* 47, 100909. doi: 10.1016/j.dcn.2020.100909

Peña, C. J., Kronman, H. G., Walker, D. M., Cates, H. M., Bagot, R. C., Purushothaman, I., et al. (2017). Early life stress confers lifelong stress susceptibility in mice via ventral tegmental area OTX2. *Science* 356, 1185–1188. doi: 10.1126/science.aan4491

Peña, C. J., Nestler, E. J., and Bagot, R. C. (2019a). Environmental Programming of Susceptibility and Resilience to Stress in Adulthood in Male Mice. *Frontiers in Behavioral Neuroscience* 13, 272. doi: 10.3389/fnbeh.2019.00040

Peña, C. J., Smith, M., Ramakrishnan, A., Cates, H. M., Bagot, R. C., Kronman, H. G., et al. (2019b). Early life stress alters

transcriptomic patterning across reward circuitry in male and female mice. *Nature Communications* 10, 5098. doi: 10.1038/s41467-019-13085-6

Pulecio, J., Verma, N., Mejía-Ramírez, E., Huangfu, D., and Raya, A. (2017). CRISPR/Cas9-Based Engineering of the Epigenome. *Cell Stem Cell* 21, 431–447. doi: 10.1016/j.stem.2017.09.006

Pusalkar, M., Suri, D., Kelkar, A., Bhattacharya, A., Galande, S., and Vaidya, V. A. (2015). Early stress evokes dysregulation of histone modifiers in the medial prefrontal cortex across the life span. *Developmental Psychobiology*, n/a-n/a. doi: 10.1002/dev.21365

Russo, S. J., and Nestler, E. J. (2013). The brain reward circuitry in mood disorders. *Nature Reviews Neuroscience* 14, 609–625. doi: 10.1038/nrn3381

Samuels, B. A., and Hen, R. (2011). "Novelty-Suppressed Feeding in the Mouse," in *Mood and Anxiety Related Phenotypes in Mice*, (Totowa, NJ: Humana Press), 107–121. doi: 10.1007/978-1-61779-313-4_7

Savell, K. E., Bach, S. V., Zipperly, M. E., Revanna, J. S., Goska, N. A., Tuscher, J. J., et al. (2019). A Neuron-Optimized CRISPR/dCas9 Activation System for Robust and Specific Gene Regulation. eNeuro 6. doi: 10.1523/ENEURO.0495-18.2019

Savolainen, M. H., Richie, C. T., Harvey, B. K., Männistö, P. T., Maguire-Zeiss, K. A., and Myöhänen, T. T. (2014). The beneficial effect of a prolyl oligopeptidase inhibitor, KYP-2047, on alpha-synuclein clearance and autophagy in A30P transgenic mouse. *Neurobiology of Disease* 68, 1–15. doi: 10.1016/j.nbd.2014.04.003

Saxton, K., and Chyu, L. (2019). Early life adversity increases the salience of later life stress: an investigation of interactive effects in the PSID. *Journal of developmental origins of health and disease* 147, 1–12. doi: 10.1017/S2040174419000308

Scott, K. M., McLaughlin, K. A., Smith, D. A. R., and Ellis, P. M. (2012). Childhood maltreatment and DSM-IV adult mental disorders: comparison of prospective and retrospective findings. *The British Journal of Psychiatry* 200, 469–475. doi: 10.1192/bjp.bp.111.103267

Seckl, J. R., Yau, J., and Holmes, M. (2002). 11Beta-hydroxysteroid dehydrogenases: a novel control of glucocorticoid action in the brain. *Endocrine research* 28, 701–707.

Shepard, R. D., Gouty, S., Kassis, H., Berenji, A., Zhu, W., Cox, B. M., et al. (2018). Targeting histone deacetylation for recovery of maternal deprivation-induced changes in BDNF and AKAP150 expression in the VTA. *Experimental Neurology* 309, 160–168. doi: 10.1016/j.expneurol.2018.08.002

Shepard, R. D., Langlois, L. D., Authement, M. E., and Nugent, F. S. (2020). Histone deacetylase inhibition reduces ventral tegmental area dopamine neuronal hyperexcitability involving AKAP150 signaling following maternal deprivation in juvenile male rats. *Journal of Neuroscience Research* 98, 1457–1467. doi: 10.1002/jnr.24613

Shepard, R. D., and Nugent, F. S. (2020). Early Life Stress- and Drug-Induced Histone Modifications Within the Ventral Tegmental Area. *Front. Cell Dev. Biol.* 8. doi: 10.3389/fcell.2020.588476

Sidamon-Eristoff, A. E., Cohodes, E. M., Gee, D. G., and Peña, C. J. (2022). Trauma exposure and mental health outcomes among Central American and Mexican children held in immigration detention at the United States–Mexico border. *Developmental Psychobiology* 64, e22227. doi: 10.1002/dev.22227

Spyrka, J., Gugula, A., Rak, A., Tylko, G., Hess, G., and Blasiak, A. (2020). Early life stress-induced alterations in the activity and morphology of ventral tegmental area neurons in female rats. *Neurobiology of Stress* 13, 100250. doi: 10.1016/j.ynstr.2020.100250

Sun, H., Damez-Werno, D. M., Scobie, K. N., Shao, N. yi, Dias, C., Rabkin, J., et al. (2015). ACF chromatin-remodeling complex mediates stress-induced depressive-like behavior. *Nature medicine* 21, 1146–1153. doi: 10.1038/nm.3939

Torres-Berrío, A., Estill, M., Ramakrishnan, A., Kronman, H., Patel, V., Minier-Toribio, A., et al. (2023). Monomethylation of Lysine 27 at Histone 3 Confers Lifelong Susceptibility to Stress. Neuroscience. doi: 10.1101/2023.05.08.539829

Wang, H., Cao, R., Xia, L., Erdjument-Bromage, H., Borchers, C., Tempst, P., et al. (2001). Purification and Functional Characterization of a Histone H3-Lysine 4-Specific Methyltransferase. *Molecular Cell* 8, 1207–1217. doi: 10.1016/S1097-2765(01)00405-1

Willmore, L., Minerva, A. R., Engelhard, B., Murugan, M., McMannon, B., Oak, N., et al. (2023). Overlapping representations of food and social stimuli in mouse VTA dopamine neurons. *Neuron*. doi: 10.1016/j.neuron.2023.08.003

Xiao, B., Jing, C., Wilson, J. R., Walker, P. A., Vasisht, N., Kelly, G., et al. (2003). Structure and catalytic mechanism of the human histone methyltransferase SET7/9. *Nature* 421, 652–656. doi: 10.1038/nature01378

Yohn, C., Dieterich, A., Bazer, A., Maita, I., Giedraitis, M., and Samuels, B. (2019). Chronic Non-Discriminatory Social Defeat Is an Effective Chronic Stress Paradigm for Both Male and Female Mice. *Neuropsychopharmacology* 44, 2220–2229. doi: 10.1038/s41386-019-0520-7

Zhang, Z.-Y., Mao, Y., Feng, X.-L., Zheng, N., Lü, L.-B., Ma, Y.-Y., et al. (2016). Early adversity contributes to chronic stress induced depression-like behavior in adolescent male rhesus monkeys. *Behavioural Brain Research* 306, 154–159. doi: 10.1016/j.bbr.2016.03.040

Supplemental Figure 1

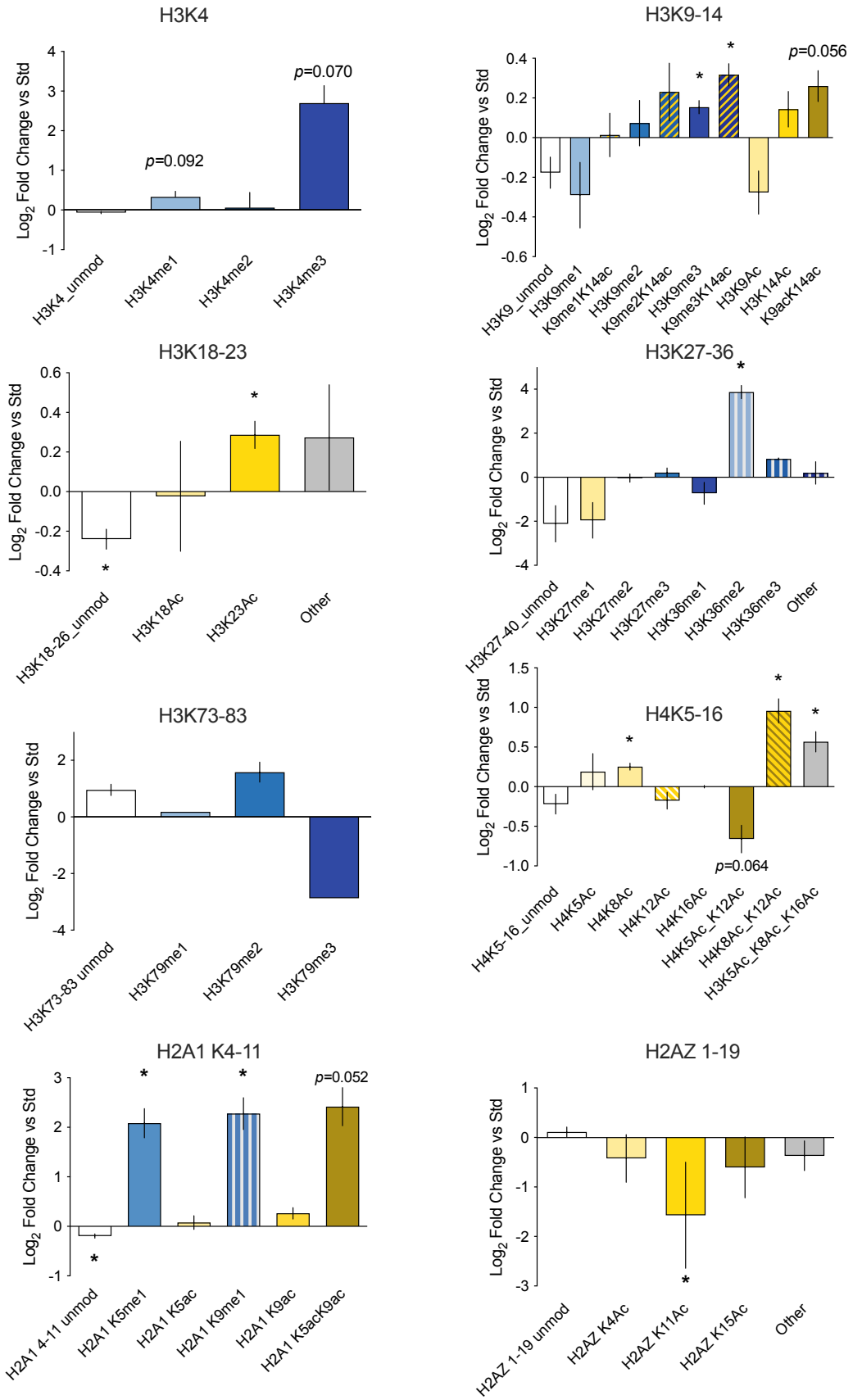

Supplemental Figure 1: Pairwise Change in PTHMs in the VTA following ELS.
Log_2 fold-change of PTHM's within each histone fragment, normalized to Std. Data are represented as mean ± SEM with two-tailed t-tests represented by *p<0.05; p values <0.1 are shown.